

Synchronization analysis between exchange rates on the basis of purchasing power parity using the Hilbert transform

Makoto Muto *

College of Economics, Nihon University

Yoshitaka Saiki †

Graduate School of Business Administration, Hitotsubashi University

*Kanda-Misakicho 1-3-2, Chiyoda-ku, Tokyo 101-8360, Japan. *E-mail:*
muto.makoto@nihon-u.ac.jp.

†Corresponding author. Naka 2-1, Kunitachi-shi, Tokyo 186-8601, Japan. *E-mail:*
yoshi.saiki@r.hit-u.ac.jp

Abstract

Synchronization is a phenomenon in which a pair of fluctuations adjust their rhythms when interacting with each other. We measure the degree of synchronization between the U.S. dollar (USD) and euro exchange rates and between the USD and Japanese yen exchange rates on the basis of purchasing power parity (PPP) over time. We employ a method of synchronization analysis using the Hilbert transform, which is common in the field of nonlinear science. We find that the degree of synchronization is high most of the time, suggesting the establishment of PPP. The degree of synchronization does not remain high across periods with economic events with asymmetric effects, such as the U.S. real estate bubble.

Key words: Synchronization, Hilbert transform, Band-pass filter, Exchange rate, U.S. dollar, Euro, Japanese yen, Purchasing power parity

JEL Classifications: C02, C14, C65, F31

1 Introduction

Exchange rates are attributed to various theories, such as purchasing power parity (PPP) (Cassel, 1918) and interest rate parity (IRP) (Keynes, 1923).¹ These theories hold for different time scales; PPP is a long-term theory, whereas IRP is a short-term theory. If PPP holds, then the exchange rate adjusts a deviation from the PPP level within several years. (see Rogoff, 1996). Ito (1997) and Taylor (2002) apply a unit root test to real exchange rates. Hasan (2006) applies a unit root test and a cointegration test to the real exchange rate of Australia and Canada. Each study shows that the deviation tends to take several years to adjust to the PPP level depending on the data. Enders and Hum (1994), Sarno (1997), Ogawa and Kawasaki (2008), and Mishra and Sharma (2010) analyze long-term equilibrium values of PPP for multiple real exchange rates.

However, the degree to which the exchange rate theory holds may differ between periods. In other words, the exchange rate adjusts to the equilibrium value indicated by the theory in a certain period but does not during other periods. Thus, this study quantifies the degree to which the exchange rate theory holds in each period. We focus on exchange rate synchronization on the basis of PPP.² Synchronization is a phenomenon in which a pair of fluctuations adjust their rhythms when interacting with each other; that is, the phase difference between the two fluctuations remains constant during a certain time interval. Approximately, phase denotes a specific position $(-\pi, \pi]$ in one amplitude of a large fluctuation. The synchronization analysis quantifies the degree of rhythm adjustment between two time series. The following studies apply the synchronization concept to economic analysis. Flood and Rose (2010), Ikeda *et al.* (2013), and Esashi *et al.* (2018) apply synchronization to study business cycles (see Onozaki, 2018). Vodenska *et al.* (2016) perform a synchronization analysis to examine the interaction and lead-lag relationship between the stock market and the foreign exchange market. Wälti (2011) investigates the relationship between stock market co-movements and monetary integration.

When two numeraire-denominated exchange rates synchronize around the

¹In addition to PPP and IRP, the flexible-price monetary model (Frenkel, 1976) and sticky-price monetary model (Dornbusch, 1976) are used. Appendix A provides additional information on the theory of exchange rate determination.

²IRP analysis requires high-frequency tick data and will be a future task due to data constraints.

PPP level, we consider that the ratio of the two data adjusts to the original exchange rate's PPP level. Therefore, the degree of synchronization measures the impact of PPP on the original exchange rate. The impact of PPP denotes the strength at which the exchange rate adjusts to the PPP level. If factors other than PPP significantly impact exchange rates, then the impact of PPP can be small.

The U.S. dollar (USD) and euro (EUR) and the USD and Japanese yen (JPY) exchange rate are analyzed. A monetary authority's foreign exchange intervention hinders theory establishment, and mutual influence is necessary in this analysis. The USD, EUR, and JPY are the three most traded currencies and have floating exchange rate systems.

The linkages between the exchange rate and international monetary policy or the degree of openness of international capital markets are now summarized. Linkages between exchange rates may occur even for currencies of countries with less freedom of capital movement and less degree of openness in their international capital markets. However, such linkages are not the subject of our analysis. For example, we consider a country with a fixed exchange rate system (dollar pegged) in which the degree of freedom of capital movement and the openness of international capital markets are low to maintain the currency system. The regulation of capital transactions hinders the establishment of PPP; however, a strong linkage occurs between the country's currency and the dollar. However, this linkage is the result of government intervention and does not underlie the PPP that is the subject of this analysis. Therefore, the currencies in our analysis should be from countries with less government regulation or exchange rate intervention because such a linkage between exchange rates suggests a theoretical background, such as PPP. The United States, the euro area, and Japan fall into this category because of their freedom of capital movement and open international capital markets.

Our analysis shows that the degree of synchronization is stably high between the USD and EUR and between the USD and JPY during certain periods.³ This result suggests that the USD/EUR and USD/JPY exchange rates adjust to PPP during the period. During other periods, the degree of synchronization does not maintain a high level for either the USD/EUR or USD/JPY. This result suggests that certain factors other than PPP affect

³More precisely, it is the synchronization between the deviations in the exchange rate from the PPP of numeraire-denominated USD and EUR, or that of the denominated USD and JPY. See section 4.3.

the exchange rate during a period.

The remainder of this paper is structured as follows. Section 2 defines synchronization, and Section 3 explains the data used in this analysis. Section 4 provides calculations of exchange rate deviation from PPP and introduces a frequency-based filter. Section 5 conducts a synchronization analysis using the Hilbert transform. Section 6 provides the results of the synchronization analysis. Section 7 discusses the difference between a synchronization analysis and the correlation coefficient. Finally, Section 8 concludes our paper.

2 Synchronization

[Figure 1 about here.]

Synchronization is a phenomenon in which a pair of fluctuations adjust their rhythms through mutual interactions. Rhythm adjustment indicates that the phase difference between two time series adjusts to remain constant for a certain time interval. We use the notion of phase to capture the degree of synchronization. The synchronization concept is explained using the simple vibrations, $f(t) = \sin(2\pi t) + 5$ and $g(t) = 2 \sin(2\pi(t - 0.25)) + 5$ [Figure 1(a)]. Phase represents a specific position $(-\pi, \pi]$ in one amplitude of oscillation data.⁴ The phases of $f(t)$ and $g(t)$ are $2\pi t$ and $2\pi(t - 0.25)$, respectively, in which each phase is converted into $(-\pi, \pi]$ value. Two time series, namely, $f(t)$ and $g(t)$, are synchronized if the phase difference is constant in time. This synchronization is called phase synchronization. In the previous case, the phase difference is $0.5n$ for all t , which are synchronized. In the Figure 1(b) illustrates the ratio of two synchronized time series, whose ratio $\frac{2 \sin(2\pi(t - 0.25)) + 5}{\sin(2\pi t) + 5}$ fluctuates around a reference value of approximately 1. In other words, this ratio has the property of returning to the reference value. This property is used to quantify the strength of the exchange rate returning to the PPP level.

3 Data

Monthly average nominal exchange rate data for the USD/EUR, USD/JPY, Australian dollar (AUD)/USD, AUD/EUR, AUD/JPY, New Zealand dollar

⁴For details, see Section 5.1 for the definition of the phase.

(NZD)/USD, NZD/EUR, and NZD/JPY during 1999:01–2017:12, 1987:01–2017:12, 1999:01–2017:12, 1999:01–2017:12, 1987:01–2017:12, 1999:01–2017:12, 1999:01–2017:12, and 1987:01–2017:12, respectively, are used. These data are obtained from *Datastream*. Monthly producer price index data are used as the price level data of the United States, the euro area, and Japan, for which 2010 data are normalized to 100. These data are obtained from the *International Financial Statistics* of the International Monetary Fund (IMF) website. Current account balances (percent of GDP) of the United States, the euro area, and Japan are yearly data obtained from the *World Economic Outlook* of the IMF website.

4 PPP and frequency band

4.1 PPP

The PPP level is calculated as

$$\rho_t^{USDj} = S_{base}^{USDj} \frac{P_t^j / P_{base}^j}{P_t^{USD} / P_{base}^{USD}}, \quad (1)$$

where S_t^{USDj} denotes the USD/currency j ($j = \text{EUR, JPY}$) exchange rate at time t , S_{base}^{USDj} denotes the USD/currency j ($j = \text{EUR, JPY}$) exchange rate at a base time, P_t^j denotes the country of currency j 's price index at time t , and P_{base}^j denotes the country of currency j 's price index at the base time. To calculate PPP, the base time is selected when the current account balances are close to zero, ρ_t^{USDEUR} is in 2010, and ρ_t^{USDJPY} is in 1991. Exchange rate fluctuations around PPP are calculated as

$$\xi_t^{USDj} := \frac{S_t^{USDj}}{\rho_t^{USDj}}. \quad (2)$$

Figure 2(a) represents the USD/EUR exchange rate and PPP level. When the USD/EUR exchange rate deviates from the PPP level, it returns to its level in approximately one to five years. Since 2015, the exchange rate has deviated from the PPP level. Figure 2(b) represents the divergence of the USD/EUR exchange rate from PPP, which fluctuates around 1. Similarly, Figure 2(c) represents the USD/JPY exchange rate and PPP level. The USD/JPY exchange rate returns to the PPP level approximately every two to

five years. In addition, the return time is longer than that of the USD/EUR exchange rate. Since 2013, the exchange rate has deviated from the PPP level. Figure 2(d) represents the divergence of the USD/JPY exchange rate from the PPP level, which fluctuates around 1.

[Figure 2 about here.]

4.2 Power spectrum

Exchange rates have many determinants other than PPP. If data contain fluctuations of various sizes, then the appropriate phase cannot be clearly defined. Therefore, identifying the frequency band that holds PPP and generates data with the frequency is needed. The power spectrum is used to identify the frequency band of the exchange rate fluctuation around PPP. See Appendix B Eq. (26) for the definition of the power spectrum. Figure 3(a) shows the log power of ξ_t^{USDEUR} , where the horizontal axis represents the monthly frequency. For example, the leftmost part of the figure suggests that a frequency component with amplitude 228 months has the highest power. The arrow represents the band used in this analysis. Figure 3(b) shows the log power of ξ_t^{USDJPY} .

The power spectrum implies that the USD/EUR exchange rate fluctuates around PPP in frequencies ranges of approximately 32.6–228.0 and 38.0–228.0 months. Then, the time series is extracted with the frequency band of that range using the lower cutoff frequency of $k_0 = 1$ and upper cutoff frequency of $k_1 = 7$, corresponding to 228.0 ($\approx 228/k_0$) and 32.6 ($\approx 228/k_1$) months, respectively. (See Appendix B for the definition of k_0 and k_1 .) Thus, if PPP holds, then deviations of the USD/EUR exchange rate from PPP have vanished from 16.3 (32.6/2) to 114.0 (228.0/2) months. Therefore, in the USD/EUR analysis, we focus on the range of the frequency band of 32.6–228.0 and 38.0–228.0 months. Similarly, the corresponding frequency bands of 37.2–186.0 or 41.3–186.0 months are expected for the USD/JPY exchange rate. Thus, if PPP holds, then the USD/JPY exchange rate deviations from PPP vanish from 18.6 (37.2/2) to 93.0 (186.0/2) months. We focus on 37.2–186.0 and 41.3–86.0 months as the frequency band in the USD and JPY analysis. The band movements are considered to represent price adjustments through trade and productivity adjustments.

[Figure 3 about here.]

4.3 Numeraire

We analyze the synchronization between fluctuations in the USD and currency j of ξ_t^{USDj} using the numeraire to divide ξ_t^{USDj} into USD and currency j parts. Then, the synchronization between these two time series is studied. Frankel and Wei (1994) and McKinnon and Schnabl (2004) adopted this method to analyze the linkage between multiple exchange rates using numeraire-denominated exchange rates.

ξ_t^{USDj} can be written using the AUD numeraire as⁵

$$\xi_t^{USDj} \approx \frac{\xi_t^{AUDj}}{\xi_t^{AUDUSD}} = \frac{\frac{S_t^{AUDj}}{S_{base}^{AUDj}(P_t^j/P_{base}^j)}}{\frac{S_t^{AUDUSD}}{S_{base}^{AUDUSD}(P_t^{USD}/P_{base}^{USD})}} = \frac{\xi_t'^{AUDj}}{\xi_t'^{AUDUSD}}, \quad (3)$$

where

$$\xi_t'^{AUDUSD} := \frac{S_t^{AUDUSD}}{S_{base}^{AUDUSD}(P_t^{USD}/P_{base}^{USD})},$$

and

$$\xi_t'^{AUDj} := \frac{S_t^{AUDj}}{S_{base}^{AUDj}(P_t^j/P_{base}^j)}.$$

$\xi_t'^{AUDUSD}$ ⁶ and $\xi_t'^{AUDj}$ exclude the AUD inflation rate from ξ_t^{AUDUSD} and ξ_t^{AUDj} . When $\xi_t'^{AUDUSD}$ and $\xi_t'^{AUDj}$ have the same fluctuation, ξ_t^{USDj} fluctuates around 1 (see Figure 1), thus suggesting the establishment of PPP.

4.4 Band-pass filter

We extract a frequency band of a numeraire-denominated exchange rate using PPP as previously described. Time series data are generated with a frequency

⁵Numeraire often uses the currency of the floating exchange rate system. The Swiss franc (CHF) and NZD are also often used for numeraire. We do not use the CHF because Swiss National Bank sets minimum exchange rate at CHF 1.20 per EUR from 2011 to 2015. Changing the NZD to numeraire does not affect the result. See Appendix C for details.

⁶ ξ_t' is not PPP in a strict sense because it excludes the inflation rate of numeraire. However, we use ξ_t' because of the small sample size of the PPI data of Australia. As shown in Eq. (3), this condition does not affect the analysis because the ξ_t' ratio is the same as that of ξ_t .

estimated from each $\xi_t^{\prime AUDUSD}$ and $\xi_t^{\prime AUDj}$ using a band-pass filter.⁷ Figure 4(a) shows $\eta_t^{\prime AUDUSD}$ and $\eta_t^{\prime AUDEUR}$ with a 32.6–228.0-month band-pass filter applied to $\xi_t^{\prime AUDUSD}$ and $\xi_t^{\prime AUDEUR}$. The two time series fluctuation rhythms do not adjust around year 2015 but in other periods. The two time series fluctuation rhythms do not adjust around 2015 but do so during other periods. Figure 4(b) indicates $\eta_t^{\prime AUDUSD}$ and $\eta_t^{\prime AUDEUR}$ with a 38.0–228.0-month band-pass filter applied to $\xi_t^{\prime AUDUSD}$ and $\xi_t^{\prime AUDEUR}$. The fluctuation rhythms of the two time series do not adjust around 2006 but do so during other periods. Figure 4(c) shows $\eta_t^{\prime AUDUSD}$ and $\eta_t^{\prime AUDJPY}$ with a 37.2–186.0-month band-pass filter applied to $\xi_t^{\prime AUDUSD}$ and $\xi_t^{\prime AUDJPY}$. The two time series fluctuation rhythms adjust around 2001 but do not do so during other periods. Figure 4(d) shows $\eta_t^{\prime AUDUSD}$ and $\eta_t^{\prime AUDJPY}$ with a 41.3–186.0-month band-pass filter applied to $\xi_t^{\prime AUDUSD}$ and $\xi_t^{\prime AUDJPY}$. The two time series fluctuation rhythms adjust around 2001 but do not do so during other periods.

[Figure 4 about here.]

5 Synchronization analysis using the Hilbert transform

5.1 Hilbert transform and instantaneous phase

In this paper, the Hilbert transform is used in our synchronization analysis to define a phase at each time. Some previous studies applied the Hilbert transform to an analysis of macroeconomic data. Ikeda *et al.* (2013) analyze the business cycle in Japan using Indices of Industrial Production (IIP) data for 16 industrial sectors. They use the Hilbert transform to calculate phases from the data and find a partial phase synchronization of Japan’s business cycles. Vodenska *et al.* (2016) study the interactions between global equity and foreign exchange markets by analyzing daily price data for foreign exchange markets and major stock indices for 48 countries. They use the complex Hilbert principal component analysis (CHPCA), which is a complex version

⁷See Appendix B for the band-pass filter details. Rodriguez *et al.* (1999) and Varela *et al.* (2001) perform a synchronization analysis using band-pass-filtered data for brain science research. Business cycle studies often use band-pass-filtered economic time series data (Baxter and King, 1999; Calderón *et al.*, 2007).

of principal component analysis that uses Hilbert transformed values for the imaginary part of the complex time series. They show that the information on lead-lag relationships in financial markets and exchange rates obtained by CHPCA can serve as an early warning system (EWS) against systemic risk contagion. The Hilbert transform is also applied to analyses in the finance field. Fusai *et al.* (2016) proposed the Wiener-Hopf factorization of complex functions that can be applied to the pricing of barrier and look-back options when monitoring is discrete. This method uses the Hilbert and z-transforms. Phelan *et al.* (2018) modify the pricing of options pricing using the discrete monitoring proposed by Fusai *et al.* (2016) when monitoring is continuous. In addition, they examine the truncation error of the sinc-based Hilbert transform to investigate the error of the pricing method. Phelan *et al.* (2019) improve the option pricing method using the sinc-based Hilbert transform with a spectral filter. This method can be applied to, for example, the pricing of barrier options when monitoring is discrete. Phelan *et al.* (2020) presents new pricing methods for Bermuda, American, and α -quantile options that use the Hilbert transforms, which have the advantage of small errors and fast CPU time.

We define a phase to measure the phase difference and assume that η_t^{AUDUSD} and η_t^{AUDj} are obtained from the real part of the complex variable data. The imaginary part of the complex data can be generated using the Hilbert transform value of the real part. The Hilbert transform can be realized by an ideal filter, for which the amplitude and phase responses are unity and a constant $\pi/2$ lag at all Fourier frequencies (Pikovsky *et al.* (2001), pp. 362-363). The Hilbert transform is expressed as

$$s_t^H = \frac{1}{\pi} P.V. \int_{-\infty}^{\infty} \frac{s_\tau}{t - \tau} d\tau, \quad (4)$$

where s_t denotes the time series data at time t and $P.V.$ denotes the Cauchy principal value integrals. A complex valued time series \hat{s}_t is constructed whose real part is actual data s_t , and the imaginary part s_t^H is generated from s_t using the Hilbert transform:

$$\hat{s}_t = s_t + s_t^H i. \quad (5)$$

The frequency spectrum of the complex number is as follows:

$$\hat{S}(f) = \begin{cases} 2S(f) & f > 0 \\ S(f) & f = 0 \\ 0 & f < 0 \end{cases} \quad (6)$$

where $\hat{S}(f)$ is the Fourier transform of \hat{s}_t , and $S(f)$ is the Fourier transform of s_t . We compute the \hat{s}_t using forward and inverse Fourier transforms. Specifically, the formula is as follows:

$$\hat{s}_t = F^{-1}(S(f)2U) = s_t + s_t^H i \quad (7)$$

where F^{-1} is an inverse Fourier transform, and U is the unit step function.⁸ This calculation provides the Hilbert transform value s_t^H .

Phase is defined by the angle ϕ_t formed by the horizontal axis and complex variable data

$$\phi_t = \begin{cases} \tan^{-1}\left(\frac{s_t^H}{s_t}\right) & (st > 0) \\ \tan^{-1}\left(\frac{s_t^H}{s_t}\right) + \pi & (st < 0) \end{cases} \quad (8)$$

Phase at a certain time is called an instantaneous phase. The value can be discontinuous over time because it ranges from $-\pi$ to π . Figure 5(a) shows that $s_t = \sin(2\pi t)$, and its Hilbert transform value $s_t^H = \sin(2\pi(t - 0.25))$, which implies $s_t^H = s_{t-\frac{\pi}{2}}$. Figure 5(b) shows a behavior of (s_t, s_t^H) in a complex plane.⁹ Phase is identified by the angle ϕ_t formed by the real axis and complex variable data.

[Figure 5 about here.]

Figures 6(a) and (b) show the behavior of (s_t, s_t^H) , where $s_t = \eta_t' AUDUSD$ and $\eta_t' AUDEUR$ with 32.6–228.0 months, respectively. Figures 6(c) and (d) show the behavior of (s_t, s_t^H) , where $s_t = \eta_t' AUDUSD$ and $\eta_t' AUDJPY$ with 37.2–186.0 months, respectively.

[Figure 6 about here.]

Figures 7(a)–(d) show instantaneous phases of 32.6–228.0, 38.0–228.0, 37.2–186.0, and 41.3–186.0 months for $\eta_t' AUDUSD$ and $\eta_t' AUDEUR$, $\eta_t' AUDUSD$

⁸We use the python program “scipy.signal.Hilbert” to obtain the Hilbert transform value from this calculation. This approach can be further refined with a sinc functions expansion yielding exponential rather than polynomial convergence of the error on the grid size, as explained in Fusai *et al.* (2016).

⁹An outlier occurs at both ends of the Hilbert transform values when numerical computations are performed. Thus, certain complex variable data near $(0, -1)$ in the complex plane deviate slightly from the unit circle. Therefore, we exclude 10 data points from both ends in the following analysis.

and $\eta'_t{}^{AUDEUR}$, $\eta'_t{}^{AUDUSD}$ and $\eta'_t{}^{AUDJPY}$, and $\eta'_t{}^{AUDUSD}$ and $\eta'_t{}^{AUDJPY}$, respectively. The phase differences in Figures 7(a)–(d) are not constant around 2006 (a), 2006 (b), 2005 and 2012 (c), and 2005 (d), respectively; however, all of them are almost constant during in other periods.

[Figure 7 about here.]

Figure 7 distinguishes between periods in which the phase difference is constant and fluctuates. Phase difference discontinuity affects its analysis. Therefore, an unwrapped instantaneous phase, which is defined, is used to allow for continuous change in the time development of an instantaneous phase.

The phase difference is expressed as

$$\psi_t = \hat{\phi}_t^{AUDUSD} - \hat{\phi}_t^{AUDj}, \quad (9)$$

where $\hat{\phi}_t^{AUDUSD}$ and $\hat{\phi}_t^{AUDj}$ denote unwrapped instantaneous phases of $\eta'_t{}^{AUDUSD}$ and $\eta'_t{}^{AUDj}$ at time t , respectively. We say that $\eta'_t{}^{AUDUSD}$ and $\eta'_t{}^{AUDj}$ synchronize in the time interval $[t_0, t_1]$ if there exists a constant d and a sufficiently small positive constant ε , such that:

$$|\psi_t - d| < \varepsilon, \quad (10)$$

for $t_0 \leq \forall t \leq t_1$.

5.2 Synchronization index

The synchronization index γ^2 (Rosenblum *et al.* (2001)) is employed for the time interval $1 \leq i \leq W$ using the phase difference ψ_i at time i to measure the degree of synchronization between two time series,

$$\gamma^2 = \left(\frac{1}{W} \sum_{i=1}^W \cos \psi_i \right)^2 + \left(\frac{1}{W} \sum_{i=1}^W \sin \psi_i \right)^2, \quad (11)$$

Index γ^2 ranges from 0 to 1. When the phase difference between two time series is constant over time, ψ_i takes a constant value. Thus, γ^2 takes the value close to 1 because $(\cos \psi_i, \sin \psi_i)$ moves in the vicinity of one point on the unit circle. Therefore, if γ^2 is close to 1, then the two time series have

high degrees of synchronization. In contrast, if γ^2 is close to 0, then the degree of synchronization is low.

Figure 8 shows the expected value of synchronization index γ^2 relevant to W . When $W = 13$ is selected, the expected value of γ^2 is 0.077 and the standard deviation of γ^2 is 0.074. Therefore, if the value of ψ_i is given at random, then the synchronization index takes a value close to 0.077, which is a reference value for judging the randomness of ψ_i .

[Figure 8 about here.]

We measure the synchronization index for the time interval W at each time t ,

$$\gamma_t^2 = \left(\frac{1}{W} \sum_{i=t-p}^{t+p} \cos \psi_i \right)^2 + \left(\frac{1}{W} \sum_{i=t-p}^{t+p} \sin \psi_i \right)^2, \quad (12)$$

where $p = (W - 1)/2$ and $0 < p < t$. In the following analysis, a window size of 13 (approximately one-year period) is set.¹⁰

6 Results and interpretation

6.1 Summary of the results

Figure 9 shows the synchronization index. If this index is stably high, the degree of synchronization between $\eta_t^{\prime AUDUSD}$ (the AUD/USD exchange rate band-pass-filtered fluctuation around PPP, excluding the AUD inflation rate) and $\eta_t^{\prime AUDj}$ is high. We call the synchronization index stably high when it maintains a high for a certain period, suggesting that the USD/currency j exchange rate fluctuates around the PPP level and confirming the establishment of PPP (see Figure 1). Conversely, if the synchronization index does not maintain a high level, the degree of synchronization between $\eta_t^{\prime AUDUSD}$ and $\eta_t^{\prime AUDj}$ is low. Although the synchronization index is temporarily high, by chance, the two instantaneous phase rhythms may match. Therefore, the

¹⁰Changing the window size does not affect the result. The synchronization analysis is performed using four window sizes: 7 (approximately 0.5 year), 13 (approximately one year), 19 (approximately 1.5 years), and 25 (approximately two years). Although the amplitude magnitude is different, periods for which the synchronization index peaks do not change. In addition, periods for which the synchronization index maintains a high value do not change.

degree of synchronization in such cases is not necessarily high. A low degree of synchronization suggests that the USD/currency j exchange rate fluctuated during this period because of factors other than PPP. For example, interest rate difference affect exchange rates. If the exchange rate fluctuates due to interest rate differences, then PPP may not hold. Therefore, the two time series have a low degree of synchronization in such periods.

Figure 9(a) shows the time development of the synchronization index $\hat{\gamma}_p^2$ between η_t^{AUDUSD} and η_t^{AUDEUR} . The degree of synchronization is stably high during 2000:05–2005:08 and 2007:09–2013:04. This finding suggests that the USD/EUR exchange rate fluctuates around the PPP level in these periods. From 2002:04 to 2002:09, the degree of synchronization decreases slightly in the short term. Therefore, we consider that this period belongs to a stably high period. Similarly, from 2013:05 to 2014:07, the degree of synchronization decreases slightly. However, when we replace the numeraire, the degree of synchronization is significantly reduced (see Figure 10 in Appendix C). Therefore, this period is not stably high.

Figure 9(b) shows the time development of the synchronization index $\hat{\gamma}_p^2$ between η_t^{AUDUSD} and η_t^{AUDJPY} . The degree of synchronization is stably high during 1991:08–1997:12, 1999:04–2003:10, and 2007:09–2010:10, suggesting that the USD/JPY exchange rate fluctuates around the PPP level during this period. From these results, the degree of synchronization between η_t^{AUDUSD} and η_t^{AUDEUR} and between η_t^{AUDUSD} and η_t^{AUDJPY} is, for the most part, high. Therefore, PPP holds in the frequency band used in this analysis. The degree of synchronization is low in certain periods for two reasons. First, an economic event may have an asymmetric effect on each η_t . Second, factors other than PPP affect exchange rates. For example, exchange rates change when the interest rate difference between two countries increases.

[Figure 9 about here.]

6.2 Interpretation of the results

This section discusses the relationship between fluctuations in the synchronization indices in the previous section and economic events. First, for the synchronization index between η_t^{AUDUSD} and η_t^{AUDEUR} , the synchronization index is stably high in many periods, suggesting the establishment of PPP. However, the degree of synchronization did not remain high during

2005:09–2007:08 and after 2013:05. During 2005–2006, a housing bubble and subsequent housing market collapse occurred in the United States, and housing prices frequently fluctuated during this period. Therefore, PPP cannot explain the price index fluctuation in the United States during this period. Because an asymmetric event occurred, the degree of synchronization did not maintain a high level during 2005:09–2007:08. Since approximately 2014, the EUR has depreciated against the USD. In addition, the exchange rate from 2015 to the first half of 2017 has been approximately 1 USD = 0.9 EUR and continues to diverge from the PPP level. The exchange rate moved toward the PPP level in the second half of 2017 (Figure 2(a)). The EUR has depreciated since 2014 because of interest rate reductions, the introduction of negative interest rates, and quantitative easing by the European Central Bank. PPP may not explain these exchange rate fluctuations. During the divergence period from the PPP level this exchange rate overlapped with the period during which the degree of synchronization did not maintain a high level after 2013:05. The Lehman Brothers’ bankruptcy in 2008:09 marked the beginning of a worldwide recession. During the economic crisis, countries’ economic variables tended to move in the same direction. Therefore, the degree of synchronization was high during 2008:9 and might not have been affected by PPP.

Second, the synchronization index between $\eta'_t{}^{AUDUSD}$ and $\eta'_t{}^{AUDJPY}$ is stably high in several periods, suggesting the establishment of PPP. However, the degree of synchronization does not remain high from 1988:05 to 1991:07, approximately during 1999, from 2003:11 to 2007:08, and after 2010:11. From 1986 to 1989, Japan experienced an economic bubble, and stocks and real estate prices soared. In addition, a technology bubble occurred around 1999. These events may have hindered the establishment of PPP from 1988:06 to 1991:07 and approximately during 1999. During 2005–2006, the United States experienced a housing bubble and subsequent housing market collapse. The event period overlaps with the period during which the degree of synchronization was not high between 2003:11 and 2007:08. The Great East Japan Earthquake in 2011:03 caused violent JPY fluctuations. During this period, the JPY appreciated because of the JPY purchase for insurance claim payments following the earthquake. In addition, investors may have bought JPY in anticipation of the currency strengthening. During 2011, the degree of synchronization was low, which may have resulted from JPY fluctuations. Moreover, since 2013, the JPY has depreciated against the USD, when the exchange rate remained deviated from the PPP level (see Figure 2(c)), be-

cause of the Bank of Japan’s quantitative easing and a 2011 rebound to the highest JPY value. PPP may not explain this exchange rate fluctuation. Therefore, the degree of synchronization did not remain high after 2010:11. The Lehman Brothers collapse in 2008:09 initiated a worldwide recession. Countries’ economic variables during the economic crisis tended to move in the same direction. Therefore, the degree of synchronization was high during 2008:09 and might not have been affected by PPP.

7 Comparison with correlation coefficient

A correlation coefficient is often used in economic studies to measure the strength of the relationship between the movements of two time series. However, the time difference in phase between two synchronized time series affects correlation coefficients. In contrast, the synchronization index is not affected by the time difference in phase. Figure 10(a) shows the synchronization index and correlation coefficient between $\sin(2\pi t)$ and $\sin(2\pi(t + \Delta t))$ relevant to Δt . The synchronization index is 1 regardless of the existence of the time difference in phase. Depending on the Δt size, the correlation coefficient can take any value between -1 and 1 . The synchronization index is useful for measuring the synchronization of two time series with the time difference in phase.

[Figure 10 about here.]

If the time difference in phase of two time series does not significantly change over time or is clearly known in each period, then the correlation coefficient can be used by shifting the time series with the time difference in phase. However, an appropriate time difference is difficult to determine from our data. We compare the synchronization index and correlation coefficient with the time difference in phase between η_t^{AUDUSD} and η_t^{AUDj} . Figures 10(b) and (c) show the time series of the synchronization index and the absolute value of a correlation coefficient and that of a correlation coefficient with the time difference in phase.¹¹ The correlation coefficient is calculated using the same moving window (window size $W = 13$) as that of the synchronization index. In addition, the time difference correlation coefficient considers the time difference in phase between two time series. Figure

¹¹See Appendix D for the calculation method of the correlation coefficient with the time difference in phase.

10(b) shows the synchronization index and correlation coefficient between η_t^{AUDUSD} and η_t^{AUDEUR} from 32.6 to 228.0 months. Figure 10(c) shows the synchronization index and correlation coefficient between η_t^{AUDUSD} and η_t^{AUDJPY} from 37.2 to 186.0 months. Using these figures, when the synchronization index greatly decreases during a period, the correlation coefficient also decreases. The time series of a synchronization index and correlation coefficient sometimes behave differently when the synchronization index is stably high. An appropriate time difference in phase is difficult to identify from our data in which the lead-lag relationship varies during the short term. Thus, we employ the synchronization index.

In addition to the correlation coefficient, many other methods exist to analyze the relationship between two time series. For example, cross-correlation is often used. The differences between each of these methods and the synchronization index are as follows. Using the cross-correlation function:

$$R_\tau^{xy} = \int_{-\infty}^{\infty} x_t y_{t-\tau} dt, \quad (13)$$

we can measure the similarity between two time series x, y with time difference τ . However, we consider that the economic data used in our analysis are likely to vary in structure with economic shocks and changes in economic conditions. Therefore, we can expect that the time lag of the relationship between two time series can change over time. Identifying the time lag in advance is difficult and is the same problem as that of the correlation coefficient with the previously explained time differences. The synchronization method has an advantage in this aspect.

8 Concluding remarks

We determine that the degree of synchronization between η_t^{AUDUSD} (band-pass-filtered fluctuation around the PPP of the AUD/USD exchange rate, excluding the AUD inflation rate) and η_t^{AUDEUR} and between η_t^{AUDUSD} and η_t^{AUDJPY} are high for most times. This result suggests that PPP holds in the long term and that the PPP level is the long-term equilibrium value of the USD/EUR and USD/JPY exchange rates. However, a high degree of synchronization is not maintained for several periods. This property can be attributed to the occurrence of asymmetrical economic events and factors

other than PPP that affect the exchange rate, such as during the U.S. real estate bubble and the Great East Japan Earthquake.

Correlation coefficients are inappropriate in this study because of the frequent time difference in phase between two time series. In contrast, we use the synchronization index in our analysis to measure the synchronization degree without identifying the time difference value in phase at each time. Therefore, synchronization analysis is suitable for our study.

We are also interested in the currency that causes synchronization in each period. However, because the synchronization index cannot measure this synchronization, methods such as Granger causality are needed, which will be discussed in future work.

Acknowledgements

The authors are grateful to Prof. Eiji Ogawa and Prof. Masao Kumamoto for their insightful comments and helpful suggestions. They would like to thank the anonymous referees for helpful comments. This work was partly supported by JST PRESTO (JPMJPR16E5), JSPS KAKENHI (17K05360, 19K01593, 19KK0067 and 21K18584), Tokio Marine Kagami Memorial Foundation, and Asset Management One Co., Ltd.

Appendix A. Theories of Exchange Rate Determination

Many factors affect exchange rates. Typical examples include price levels, interest rates, and balances of payment. Here, we describe exchange rate fluctuations on the basis of these factors. As a result of international commodity arbitrage, the law of one price is established.

$$S_t^{xy} P_t^x = P_t^y. \quad (14)$$

where S_t^{xy} denotes the x/y exchange rate at time t , P_t^x denotes the price level of the country of currency x at time t , and P_t^y denotes the price level of the country of currency y at time t . The absolute PPP determines the exchange rate level from the ratio of the price levels between the two countries.

$$S_t^{xy} = \frac{P_t^y}{P_t^x}. \quad (15)$$

The relative PPP determines the rate of change in the exchange rate from the difference in inflation rates between the two countries.

$$\frac{S_t^{xy} - S_{t-1}^{xy}}{S_{t-1}^{xy}} = \dot{P}_t^y - \dot{P}_t^x. \quad (16)$$

where \dot{P}_t^x denotes inflation rate of the country of currency x at time t , and \dot{P}_t^y denotes the inflation rate of the country of currency y at time t .

The uncovered IRP determines the rate of change in the exchange rate from the difference in interest rates between the two countries.

$$\frac{S_t^{xy} - S_{t-1}^{xy}}{S_{t-1}^{xy}} = i_t^y - i_t^x. \quad (17)$$

where i_t^x denotes the interest rate of the country of currency x at time t , and i_t^y denotes the interest rate of the country of currency y at time t .

Imbalances in the balance of payments affect exchange rate fluctuations. For example, a current account surplus in the home country increases the demand for the home currency, causing the home currency to appreciate. Conversely, a home country's current account deficit increases the supply of its currency, causing the home currency to depreciate.

This paper focuses on exchange rate deviations on the basis of the relative PPP. The deviations are expected to be influenced by long-run adjustments in price levels and the productivity between the two countries. Therefore, our analysis focuses on the long-term movement of exchange rates on the basis of PPP.

Interest rates and balance of payments are also considered to affect the long-term movement of exchange rates. We follow two steps to focus mainly on the relationship between PPP and the exchange rate. First, in our analysis, we use data on exchange rate deviations from PPP. Second, we estimate the frequency band that corresponds to adjustments in the exchange rate to PPP and extract the frequency band from the data. The analysis including other factors, such as interest rates and balance of payments, is left for future work.

Appendix B. Fourier band-pass filter and power spectrum

We focus on recurrent patterns in a specific time scale to measure the degree of synchronization between two time series data. We employ a band-pass filter using a Fourier series representation and briefly review the Fourier series of function f . For simplicity, let f be a real-valued continuous periodic function on $[0, L)$. The function f can be represented as a Fourier series in Eq. (18) as

$$f(x) = \frac{a_0}{2} + \sum_{k=1}^{\infty} \left(a_k \cos\left(\frac{2\pi kx}{L}\right) + b_k \sin\left(\frac{2\pi kx}{L}\right) \right), \quad (18)$$

where

$$a_k = \frac{1}{L} \int_0^L f(x) \cos\left(\frac{2\pi kx}{L}\right) dx \quad (k = 0, 1, 2, 3, \dots), \quad (19)$$

$$b_k = \frac{1}{L} \int_0^L f(x) \sin\left(\frac{2\pi kx}{L}\right) dx \quad (k = 1, 2, 3, \dots). \quad (20)$$

We can consider the Fourier series for more general functions (e.g., Korner 2008). By taking a partial sum in Eq. (18), we can create a band-pass-filtered periodic function \tilde{f} of a given function f using bands k for $1 \leq k_0 \leq k \leq k_1$:

$$\tilde{f}(x) = \sum_{k=k_0}^{k_1} \left(a_k \cos\left(\frac{2\pi kx}{L}\right) + b_k \sin\left(\frac{2\pi kx}{L}\right) \right). \quad (21)$$

The transformation procedure from discrete non-periodic time series data $g_n = g(x_0 + n\Delta x)$ ($n = 0, \dots, N-1$) to band-pass-filtered discrete periodic time series data $\tilde{f}_n = \tilde{f}(x_0 + n\Delta x)$ ($n = 0, \dots, N-1$) is as follows.

1. Using the linear transformation determined by g_0 at x_0 and g_{N-1} at x_{N-1} , convert a given set of uniformly discretized $N+1$ time series data $(g_n)_{n=0, \dots, N-1}$ into a periodic data $(f_n)_{n=0, \dots, N-1}$ such that $f_0 = f_{N-1}$ ($= g_0$).
2. Compute Fourier coefficients a_k, b_k for $(f_n)_{n=0, \dots, N-1}$.
3. Construct a band-pass-filtered periodic time series data $(\tilde{f}_n)_{n=0, \dots, N-1}$ using a_k, b_k for k_0, k_1 ($1 \leq k_0 \leq k \leq k_1$).

Step 1

$$f_n = g_n - sx_n\Delta x \quad (n = 0, \dots, N - 1), \quad (22)$$

where $s = (g_{N-1} - g_0)/(x_{N-1} - x_0)$, $x_n = x_0 + n\Delta x$ and $\Delta x = (x_{N-1} - x_0)/(N - 1)$.

Step 2

Compute

$$a_k = \frac{1}{L} \sum_{n=0}^{N-1} f_n \cos\left(\frac{2\pi k x_n}{L}\right) \Delta x \quad (k = 0, \dots, K), \quad (23)$$

$$b_k = \frac{1}{L} \sum_{n=0}^{N-1} f_n \sin\left(\frac{2\pi k x_n}{L}\right) \Delta x \quad (k = 1, \dots, K). \quad (24)$$

Step 3

$$\tilde{f}_n = \sum_{k=k_0}^{k_1} \left(a_k \cos\left(\frac{2\pi k x_n}{L}\right) + b_k \sin\left(\frac{2\pi k x_n}{L}\right) \right). \quad (25)$$

Power spectrum: We can compute power spectrum $E(k)$ for each k ,

$$E(k) = \frac{a_k^2 + b_k^2}{2}. \quad (26)$$

If f is C^l function, then $k^l |a_k|, k^l |b_k| < \infty$, implying that the Fourier coefficients decrease exponentially as k increases. Notably, we plot $\sqrt{E(k)}$ and not $E(k)$ (Figure 3).

Appendix C. Robustness check of numeraire

The third country's currency is introduced as a numeraire to analyze the synchronization between two currencies (e.g., USD and EUR). We use the AUD as the numeraire in the main body. We confirm the same results by using NZD as the numeraire in this appendix.

Figure 11(a) shows the time development of the synchronization index from 32.6 to 228.0 months between $\eta'_t{}^{AUDUSD}$ and $\eta'_t{}^{AUDEUR}$ and between $\eta'_t{}^{NZDUSD}$ and $\eta'_t{}^{NZDEUR}$. The time series of the two synchronization indices behave similarly, except during 2014. Figure 11(b) shows the time

development of the synchronization index from 37.2 to 186.0 months between $\eta'_t{}^{AUDUSD}$ and $\eta'_t{}^{AUDJPY}$ and between $\eta'_t{}^{NZDUSD}$ and $\eta'_t{}^{NZDJPY}$. The time series of the two synchronization indices behave similarly except during 1989:05.

[Figure 11 about here.]

Appendix D. Calculation method for correlation coefficient with time difference in phase

The time difference in phase between two time series affects a correlation coefficient. Thus, the correlation coefficient is not useful when the time difference is not sufficiently small. However, the correlation coefficient may show result similar to that of the synchronization index when the time difference in phase is considered. The correlation coefficient with the time difference in phase is calculated as follows.

1. Identify the leading time series, and calculate the phase difference at each time. Find $m_t (= \hat{m}_t)$ and $q_t (= \hat{q}_t)$ that satisfy $\min_{q_t \in \mathbb{Z}} (|m_t|)$, where $m_t = \hat{\phi}_t^{AUDUSD} - \hat{\phi}_t^{AUDj} + 2q_t\pi$. The variables $\hat{\phi}_t^{AUDUSD}$ and $\hat{\phi}_t^{AUDj}$ denote unwrapped instantaneous phases of $\eta'_t{}^{AUDUSD}$ and $\eta'_t{}^{AUDj}$, respectively, both at time t .
2. Calculate the time difference in phase at each time and $\hat{l}_t = l - 1$ that satisfies

$$\begin{cases} \max_{l \in N, |l| \leq L} (\hat{\phi}_t^{AUDUSD} - \hat{\phi}_{t+l}^{AUDj} + 2\hat{q}_t\pi) < 0 & (\hat{m}_t > 0) \\ \min_{l \in N, |l| \leq L} (\hat{\phi}_{t+l}^{AUDUSD} - \hat{\phi}_t^{AUDj} + 2\hat{q}_t\pi) > 0 & (\hat{m}_t < 0) \end{cases}, \quad (27)$$

where L is chosen depending on the data. The time difference in phase at each time is expressed as

$$\delta_t = \begin{cases} \hat{l}_t + \frac{\phi_t^{AUDUSD} - \phi_{t+\hat{l}_t}^{AUDj}}{\phi_{t+\hat{l}_t+1}^{AUDj} - \phi_{t+\hat{l}_t}^{AUDj}} & (\hat{m}_t > 0) \\ \hat{l}_t + \frac{\phi_t^{AUDj} - \phi_{t+\hat{l}_t}^{AUDUSD}}{\phi_{t+\hat{l}_t+1}^{AUDUSD} - \phi_{t+\hat{l}_t}^{AUDUSD}} & (\hat{m}_t < 0) \end{cases}, \quad (28)$$

3. Compute the absolute value of the correlation coefficient with the time difference in phase

$$\hat{r}_p^2 = \begin{cases} \left| \frac{\sum_{i=t}^{t'} (\eta_i^{AUDUSD} - \bar{\eta}^{AUDUSD}) (\eta_{i+\delta_t}^{AUDj} - \bar{\eta}^{AUDj})}{\sqrt{\sum_{i=t}^{t'} (\eta_i^{AUDUSD} - \bar{\eta}^{AUDUSD})^2} \sqrt{\sum_{i=t}^{t'} (\eta_{i+\delta_t}^{AUDj} - \bar{\eta}^{AUDj})^2}} \right| & (\hat{m}_t > 0) \\ \left| \frac{\sum_{i=t}^{t'} (\eta_{i+\delta_t}^{AUDUSD} - \bar{\eta}^{AUDUSD}) (\eta_i^{AUDj} - \bar{\eta}^{AUDj})}{\sqrt{\sum_{i=t}^{t'} (\eta_{i+\delta_t}^{AUDUSD} - \bar{\eta}^{AUDUSD})^2} \sqrt{\sum_{i=t}^{t'} (\eta_i^{AUDj} - \bar{\eta}^{AUDj})^2}} \right| & (\hat{m}_t < 0) \end{cases} \quad (29)$$

where $t' = t + W + 1$, $p = t + \frac{W+1}{2}$ and $\bar{\delta}_t = \frac{1}{W} \sum_{i=t}^{t+W-1} \delta_i$. W denotes the window size.

References

- Baxter, M. and King, R.G., Measuring Business Cycles: Approximate Band-Pass Filters for Economic Time Series. *The Review of Economics and Statistics*, 1999, **81**, 575–593.
- Calderón, C., Chong, A. and Stein, E., Trade intensity and business cycle synchronization: Are developing countries any different?. *Journal of International Economics*, 2007, **71**, 2–21.
- Cassel, G., Abnormal Deviations in International Exchanges. *The Economic Journal*, 1918, **28**, 413–415.
- Dornbusch, R., Expectations and exchange rate dynamics. *Journal of political Economy*, 1976, **84**, 1161–1176.
- Enders, W. and Hum, S., Theory and Tests of Generalized Purchasing-Power Parity: Common Trends and Real Exchange Rates In the Pacific Rim. *Review of International Economics*, 1994, **2**, 179–190.

- Esashi, K., Onozaki, T., Saiki, Y. and Sato, Y., Intermittent transition between synchronization and desynchronization in multi-regional business cycles. *Structural Change and Economic Dynamics*, 2018, **44**, 68–76.
- Flood, R.P. and Rose, A.K., Inflation targeting and business cycle synchronization. *Journal of International Money and Finance*, 2010, **29**, 704–727.
- Frankel, J.A. and Wei, S.J., Yen bloc or dollar bloc? Exchange rate policies of the East Asian economies. In *Macroeconomic linkage: Savings, exchange rates, and capital flows*, pp. 295–333, 1994, University of Chicago Press.
- Frenkel, J.A., A Monetary Approach to the Exchange Rate: Doctrinal Aspects and Empirical Evidence. *The Scandinavian Journal of Economics*, 1976, **78**, 200–224.
- Fusai, G., Germano, G. and Marazzina, D., Spitzer identity, Wiener-Hopf factorization and pricing of discretely monitored exotic options. *European Journal of Operational Research*, 2016, **251**, 124–134.
- Hasan, M.S., A century of Purchasing Power Parity: evidence from Canada and Australia. *Applied Financial Economics*, 2006, **16**, 145–156.
- Ikedo, Y., Aoyama, H., Iyetomi, H. and Yoshikawa, H., Direct evidence for synchronization in Japanese business cycles. *Evolutionary and Institutional Economics Review*, 2013, **10**, 315–327.
- Ito, T., The Long-Run Purchasing Power Parity for the Yen: Historical Overview. *Journal of the Japanese and International Economies*, 1997, **11**, 502–521.
- Keynes, J.M., *A tract on monetary reform*, 1923, Macmillan and Co., limited.
- McKinnon, R. and Schnabl, G., The East Asian Dollar Standard, Fear of Floating, and Original Sin. *Review of Development Economics*, 2004, **8**, 331–360.
- Mishra, R.K. and Sharma, C., Real exchange rate behavior and optimum currency area in East Asia: Evidence from Generalized Purchasing Power Parity. *International Review of Financial Analysis*, 2010, **19**, 205–213.

- Ogawa, E. and Kawasaki, K., Adopting a common currency basket arrangement into the ASEAN plus three. In *International Financial Issues in the Pacific Rim: Global Imbalances, Financial Liberalization, and Exchange Rate Policy*, pp. 219–237, 2008, University of Chicago Press.
- Onozaki, T., *Nonlinearity, bounded rationality, and heterogeneity: Some Aspects of Market Economies as Complex Systems*, 2018, Springer.
- Phelan, C.E., Marazzina, D. and Germano, G., Pricing methods for α -quantile and perpetual early exercise options based on Spitzer identities. *Quantitative Finance*, 2020, **20**, 899–918.
- Phelan, C.E., Marazzina, D., Fusai, G. and Germano, G., Fluctuation identities with continuous monitoring and their application to the pricing of barrier options. *European Journal of Operational Research*, 2018, **271**, 210–223.
- Phelan, C.E., Marazzina, D., Fusai, G. and Germano, G., Hilbert transform, spectral filters and option pricing. *Annals of Operations Research*, 2019, **282**, 273–298.
- Pikovsky, A., Rosenblum, M. and Kurths, J., *Synchronization: A Universal Concept in Nonlinear Sciences*, 2001 (Cambridge University Press: Cambridge).
- Rodriguez, E., George, N., Lachaux, J.P., Martinerie, J., Renault, B. and Varela, F.J., Perception’s shadow: long-distance synchronization of human brain activity. *Nature*, 1999, **397**, 430–433.
- Rogoff, K., The purchasing power parity puzzle. *Journal of Economic literature*, 1996, **34**, 647–668.
- Rosenblum, M., Pikovsky, A., Kurths, J., Schäfer, C. and Tass, P.A., Phase Synchronization: From Theory to Data Analysis. In *Neuro-Informatics and Neural Modelling*, edited by F. Moss and S. Gielen, Vol. 4 of *Handbook of Biological Physics*, chap. 9, pp. 279–321, 2001 (Elsevier Science: Amsterdam).
- Sarno, L., Policy convergence, the exchange rate mechanism and the misalignment of exchange rates. Some tests of purchasing power parity and

- generalized purchasing power parity. *Applied Economics*, 1997, **29**, 591–605.
- Taylor, A.M., A Century of Purchasing-Power Parity. *The Review of Economics and Statistics*, 2002, **84**, 139–150.
- Varela, F., Lachaux, J.P., Rodriguez, E. and Martinerie, J., The brainweb: phase synchronization and large-scale integration. *Nature reviews neuroscience*, 2001, **2**, 229–239.
- Vodenska, I., Aoyama, H., Fujiwara, Y., Iyetomi, H. and Arai, Y., Interdependencies and Causalities in Coupled Financial Networks. *PloS one*, 2016, **11**.
- Wälti, S., Stock market synchronization and monetary integration. *Journal of International Money and Finance*, 2011, **30**, 96–110.

List of Figures

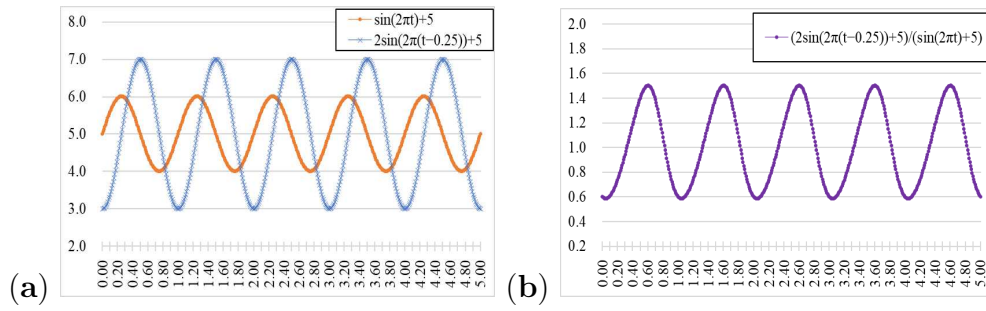


Figure 1. (a) Two phase-synchronized time series. Note: “●” (orange) represents $\sin(2\pi t) + 5$, and “×” (blue) represents $2\sin(2\pi(t - 0.25)) + 5$. The amplitudes of two time series are different. Although the phases of two time series are also different from each other, the phase difference between two time series is kept constant. (b) The ratio of the two synchronized time series. Note: “●” (purple) represents $\frac{2\sin(2\pi(t - 0.25)) + 5}{\sin(2\pi t) + 5}$. This ratio oscillates around 1.

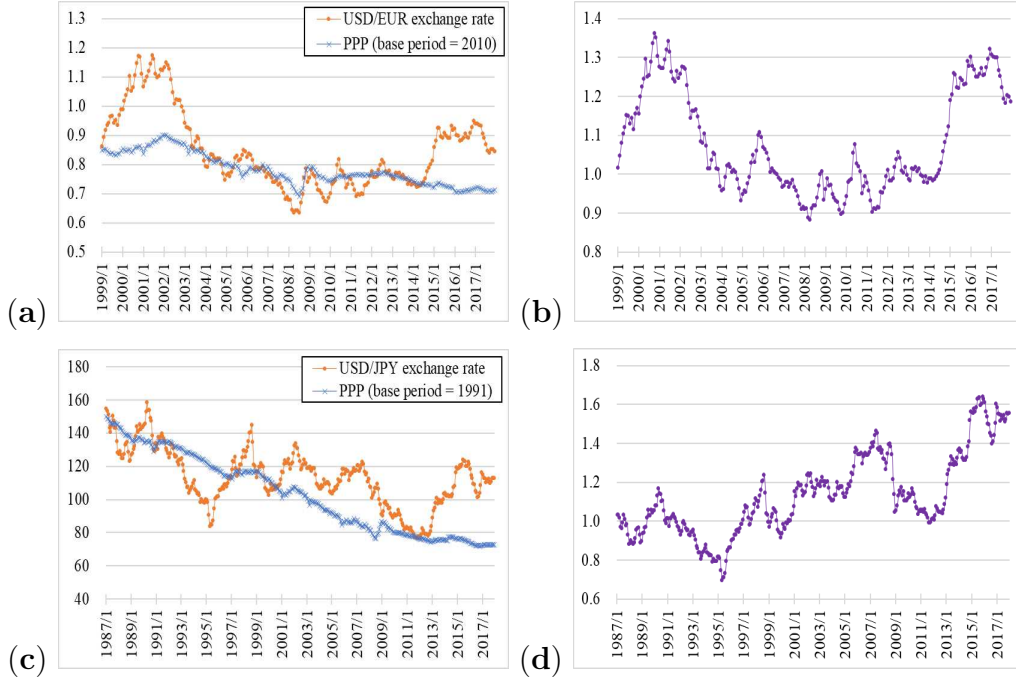


Figure 2. (a) USD/EUR exchange rate and PPP level (ρ_t^{USDEUR}). Note: “●” (orange) represents the USD/EUR exchange rate, and “×” (blue) represents the PPP level. When the USD/EUR exchange rate deviates from the PPP level, it returns to its level in approximately one to five years. (b) The exchange rate fluctuations around PPP (ξ_t^{USDEUR}). Note: “●” (purple) represents the divergence of the USD/EUR exchange rate from PPP. The value fluctuates around 1. (c) USD/JPY exchange rate and PPP level (ρ_t^{USDJPY}). Note: “●” (orange) represents the USD/JPY exchange rate, and “×” (blue) represents the PPP level. The USD/JPY exchange rate has returned to the PPP level over a long period. The USD/JPY exchange rate returns to the PPP level approximately every two to five years. (d) The exchange rate fluctuations around PPP (ξ_t^{USDJPY}). Note: “●” (purple) represents the divergence of the USD/JPY exchange rate from the PPP level. The value fluctuates around 1.

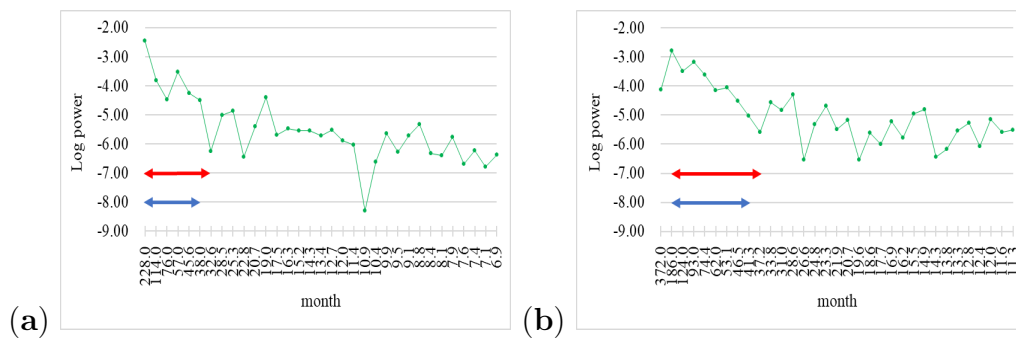


Figure 3. (a) The log power of the exchange rate fluctuations around PPP (ξ_t^{USDEUR}). Note: The horizontal axis represents monthly frequency. The arrow represents the band used in this analysis. The exchange rate fluctuations around PPP (ξ_t^{USDEUR}) oscillate in the frequency band represented by the arrows. Therefore, we expect that the USD/EUR exchange rate fluctuates around PPP in approximate frequency ranges of 32.6–228.0 and 38.0–228.0. (b) The log power of the exchange rate fluctuations around PPP (ξ_t^{USDJPY}). Note: We can expect that the USD/EUR exchange rate fluctuates around PPP (ξ_t^{USDJPY}) in the approximate frequency ranges of 37.2–186.0 or 41.3–186.0.

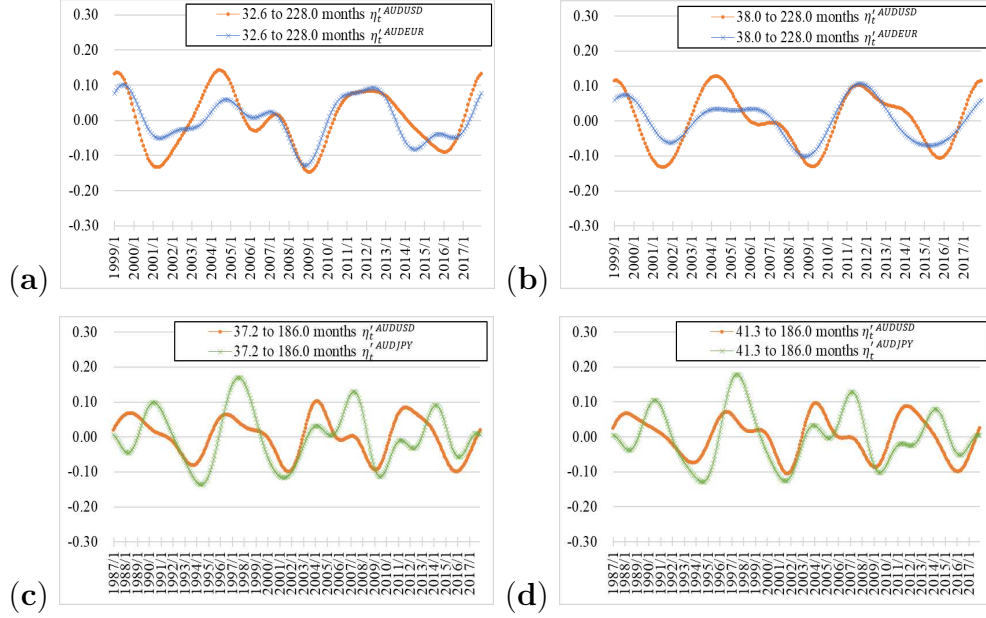


Figure 4. (a) The 32.6–228.0-month band-pass filtered data η_t^{AUDUSD} and η_t^{AUDEUR} of the exchange rate fluctuations around PPP (ξ_t^{AUDUSD} and ξ_t^{AUDEUR}). Note: The two time series fluctuation rhythms do not adjust during year 2015 but during other periods. (b) The 38.0–228.0-month band-pass filtered data η_t^{AUDUSD} and η_t^{AUDEUR} of the exchange rate fluctuations around PPP (ξ_t^{AUDUSD} and ξ_t^{AUDEUR}). Note: The two time series fluctuation rhythms do not adjust during 2006 but during other periods. (c) The 37.2–186.0-month band-pass filtered data η_t^{AUDUSD} and η_t^{AUDJPY} of the exchange rate fluctuations around PPP (ξ_t^{AUDUSD} and ξ_t^{AUDJPY}). Note: The two time series fluctuation rhythms adjust during 2001 but not during other periods. (d) The 41.3–186.0-month band-pass filtered data η_t^{AUDUSD} and η_t^{AUDJPY} of the exchange rate fluctuations around PPP (ξ_t^{AUDUSD} and ξ_t^{AUDJPY}). Note: The two time series fluctuation rhythms adjust during 2001 but not during other periods.

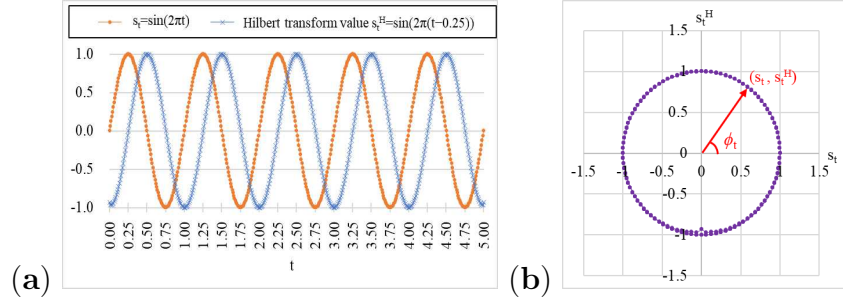


Figure 5. (a) $s_t = \sin(2\pi t)$ and its Hilbert transform value $s_t^H = \sin(2\pi(t - 0.25))$. Note: “ \times ” (blue) represents $s_t^H = \sin(2\pi(t - 0.25))$ delayed by $\pi/2$ from $s_t = \sin(2\pi t)$ and is created by the Hilbert transform. (b) Behavior of (s_t, s_t^H) on a complex plane. Note: The phase is defined by the angle ϕ_t formed by the horizontal axis and the complex variable data (s_t, s_t^H) .

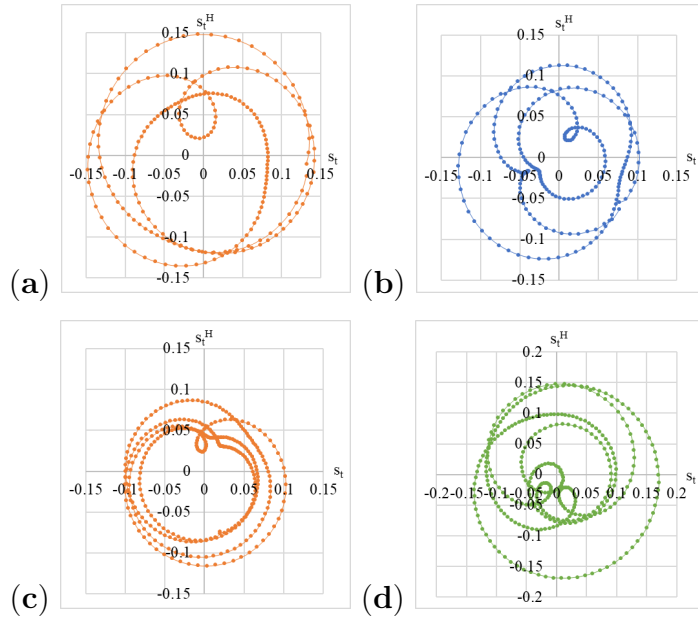


Figure 6. (a) Behavior of (s_t, s_t^H) , where $s_t = \eta_t'^{AUDUSD}$ with 32.6–228.0 months. (b) Behavior of (s_t, s_t^H) , where $s_t = \eta_t'^{AUDEUR}$ with 32.6–228.0 months. (c) Behavior of (s_t, s_t^H) , where $s_t = \eta_t'^{AUDUSD}$ with 37.2–186.0 months. (d) Behavior of (s_t, s_t^H) , where $s_t = \eta_t'^{AUDJPY}$ with 37.2–186.0 months. Note: When defining the phase, the complex data should rotate around the origin. The phase can jump when the complex data move quite close to the origin. From the figure, the complex data seem to rotate around the origin, although a few small circles are mixed in.

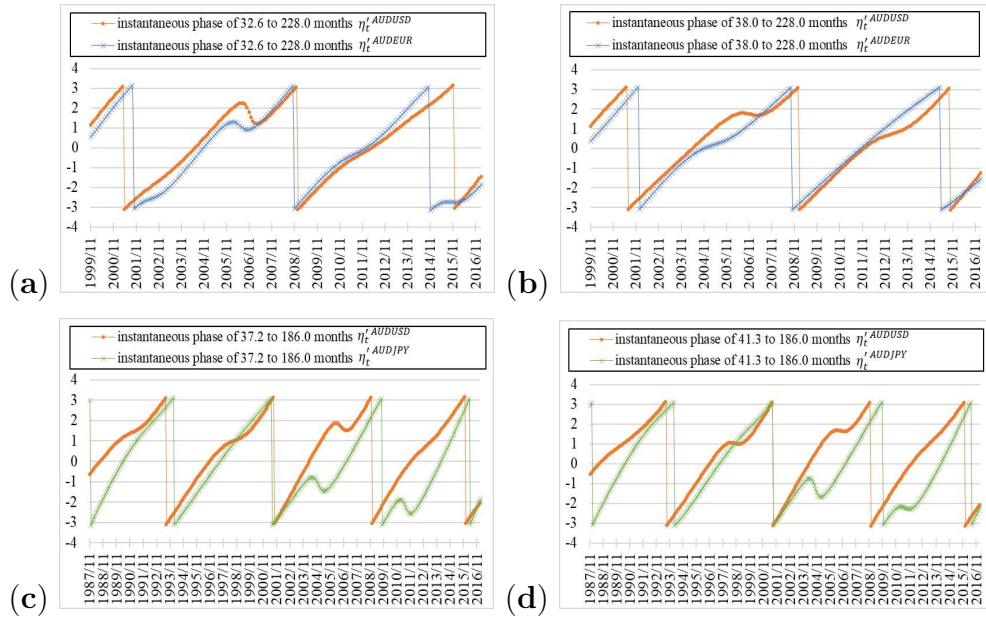


Figure 7. (a) The instantaneous phase of 32.6–228.0 months η_t^{AUDUSD} and η_t^{AUDEUR} . (b) The instantaneous phase of 38.0–228.0 months η_t^{AUDUSD} and η_t^{AUDEUR} . (c) The instantaneous phase of 37.2–186.0 months η_t^{AUDUSD} and η_t^{AUDJPY} . (d) The instantaneous phase of 41.3–186.0 months η_t^{AUDUSD} and η_t^{AUDJPY} . Note: The phase differences in Figures 7(a)–(d) are not constant around (a) 2006, (b) 2006, (c) 2005 and 2012, and (d) 2005, respectively; however, all are almost constant during other periods.

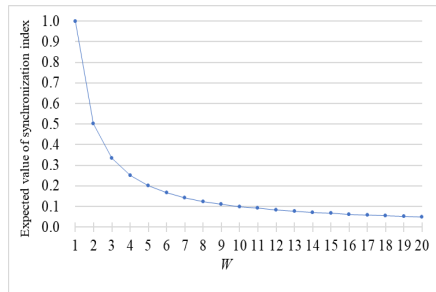


Figure 8. The expected value of the synchronization index γ^2 with respect to W calculated from 10,000 cases. ψ_i is chosen from a uniform distribution of $[0, 2\pi]$. When we select $W = 13$, the expected value of γ^2 is 0.077 and the standard deviation of γ^2 is 0.074. The synchronization index with $W = 13$ used in our analysis is small enough to include random values. Therefore, if the synchronization index is near 1, the two time series are considered to be highly synchronized.

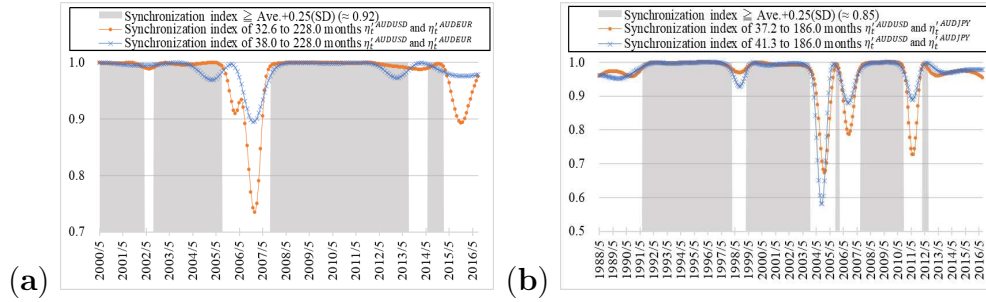


Figure 9. (a) The synchronization index between η_t^{AUDUSD} and η_t^{AUDEUR} . Note: The gray-colored interval indicates that the synchronization index from 32.6 to 228.0 months between η_t^{AUDUSD} and η_t^{AUDEUR} is the synchronization index $\gamma^2 \geq \gamma^{2*} (\approx 0.92)$, where γ^{2*} denotes (the average value) + 0.25(standard deviation). (b) The synchronization index from 37.2 to 186.0 months between η_t^{AUDUSD} and η_t^{AUDJPY} . Note: The gray-colored interval indicates that the synchronization index between η_t^{AUDUSD} and η_t^{AUDJPY} is $\gamma^2 \geq \gamma^{2*} (\approx 0.85)$.

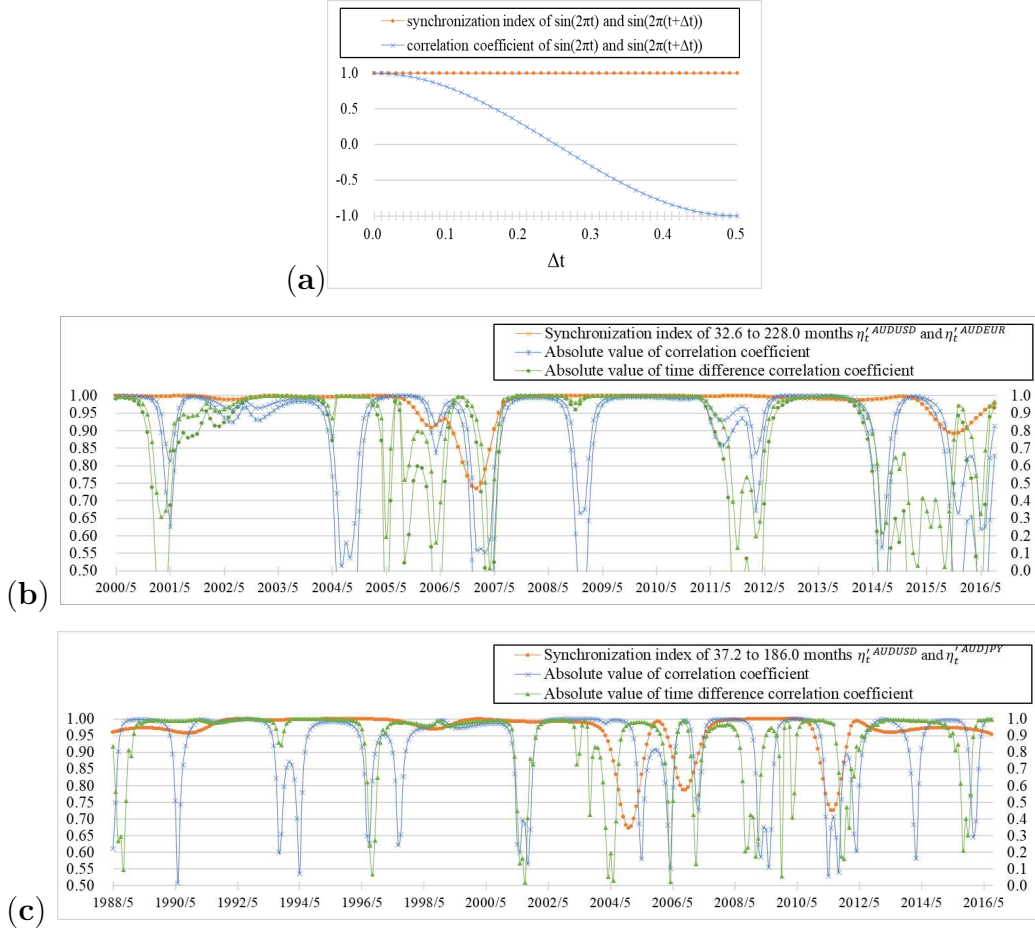


Figure 10. (a) The synchronization index and correlation coefficient between two time series $\sin(2\pi t)$ and $\sin(2\pi(t + \Delta t))$. (b) The synchronization index and correlation coefficient from 32.6 to 228.0 months between η_t^{AUDUSD} and η_t^{AUDEUR} . Note: “●” (orange), “×” (blue), and “▲” (green) represent the synchronization index, absolute value of the correlation coefficient, and absolute value of the correlation coefficient from 32.6 to 228.0 months with the time difference, respectively, between η_t^{AUDUSD} and η_t^{AUDEUR} . (c) The synchronization index and correlation coefficient from 37.2 to 186.0 months between η_t^{AUDUSD} and η_t^{AUDJPY} . Note: “●” (orange), “×” (blue), and “▲” (green) represent the synchronization index, absolute value of the correlation coefficient, and absolute value of the correlation coefficient from 37.2 to 186.0 months with the time difference, respectively, between η_t^{AUDUSD} and η_t^{AUDJPY} .

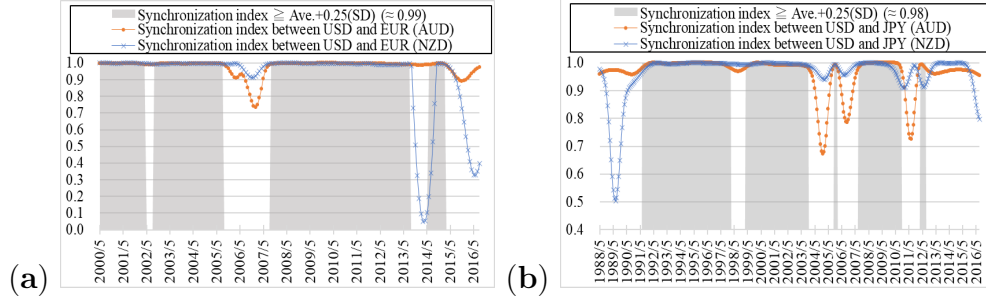


Figure 11. (a) The synchronization index between η_t^{AUDUSD} and η_t^{AUDEUR} and between η_t^{NZDUSD} and η_t^{NZDEUR} . Note: “●” (orange) and “×” (blue) represent the synchronization index from 32.6 to 228.0 months between η_t^{AUDUSD} and η_t^{AUDEUR} and between η_t^{NZDUSD} and η_t^{NZDEUR} , respectively. The gray-colored interval indicates that the synchronization index from 32.6 to 228.0 months between η_t^{AUDUSD} and η_t^{AUDEUR} is the synchronization index $\gamma^2 \geq \gamma^{2*} (\approx 0.92)$, where γ^{2*} denotes (the average value) + 0.25(standard deviation). (b) Synchronization index between η_t^{AUDUSD} and η_t^{AUDJPY} and between η_t^{NZDUSD} and η_t^{NZDJPY} . Note: “●” (orange) and “×” (blue) represent the synchronization index from 37.2 to 186.0 months between η_t^{AUDUSD} and η_t^{AUDJPY} and between η_t^{NZDUSD} and η_t^{NZDJPY} , respectively. The gray-colored interval indicates that the synchronization index from 37.2 to 186.0 months between η_t^{AUDUSD} and η_t^{AUDJPY} is $\gamma^2 \geq \gamma^{2*} (\approx 0.85)$.